# Recent developments in high-temperature photonic crystals for energy conversion

**Veronika Rinnerbauer,*[a] Sidy Ndao,[b,c] Yi Xiang Yeng,[a,b] Walker R. Chan,[a,b] Jay J. Senkevich,[b] John D. Joannopoulos,[a,b] Marin Soljačić[a,b] and Ivan Celanovic[b]**

***Received Xth XXXXXXXXXX 20XX, Accepted Xth XXXXXXXXX 20XX***
***First published on the web Xth XXXXXXXXXX 200X***
**DOI: 10.1039/b000000x**

After decades of intense studies focused on cryogenic and room temperature nanophotonics, scientific interest is also growing in high-temperature nanophotonics aimed at solid-state energy conversion. These latest extensive research efforts are spurred by a renewed interest in high temperature thermal-to-electrical energy conversion schemes including thermophotovoltaics (TPV), solar-thermophotovoltaics, solar-thermal, and solar-thermochemical energy conversion systems. This field is profiting tremendously from the outstanding degree of control over the thermal emission properties that can be achieved with nanoscale photonic materials. The key to obtaining high efficiency in this class of high temperature energy conversion is the spectral and angular matching of the radiation properties of an emitter to those of an absorber. Together with the achievements in the field of high-performance narrow bandgap photovoltaic cells, the ability to tailor the radiation properties of thermal emitters and absorbers using nanophotonics facilitates a route to achieving the impressive efficiencies predicted by theoretical studies.
In this review, we will discuss the possibilities of emission tailoring by nanophotonics in the light of high temperature thermal-to-electrical energy conversion applications, and give a brief introduction to the field of TPV. We will show how a class of large area 2D metallic photonic crystals can be designed and employed to efficiently control and tailor the spectral and angular emission properties, paving the way towards new and highly efficient thermophotovoltaic systems and enabling other energy conversion schemes based on high-performance high-temperature nanoscale photonic materials.

## 1 Introduction

Photonic crystals (PhCs) are periodically nanostructured metamaterials with extraordinary optical properties.[1–4] They exhibit a complex photonic band structure of allowed (propagating) and forbidden (decaying) states in a wavelength range comparable to the length scale of their structure. In particular, metallic photonic crystals have been shown to possess large bandgaps.[5–8] The ability to modulate the photonic density of states and hence spontaneous emission rates in metallic PhCs opens a wide range of possibilities to design and tailor thermal radiation sources.[9,10]

An ideal thermal emitter follows Planck's law of blackbody radiation. Most realistic materials are not ideal blackbody emitters but rather 'graybodies', showing less than ideal emission, depending on the bulk material properties and their geometry. To tailor thermal emission with respect to spectral, directional and polarization properties, material structuring on the subwavelength level is necessary. Photonic crystals with new absorption and emission properties can indeed be created, and their extraordinary properties enable enhanced emission approaching that of an ideal blackbody radiator, as well as tailored spectrally and directionally selective behavior. It has also been shown that photonic crystals can have narrow angular and spectral thermal radiation properties resulting in increased spatial and temporal coherence in the far field.[11–13] Thus, photonic crystals pave the way from classical isotropic, broadband and incoherent thermal radiation sources towards controlled spectrally and directionally selective, quasicoherent and highly efficient thermal radiation sources at very high operating temperatures.

This new class of highly selective absorbers and emitters enables the next generation high performance energy generation and conversion applications like solar thermal applications, concentrated thermal and thermophotovoltaics (TPV). In these thermal-to-electrical energy conversion schemes, one key factor to achieving high efficiency is the spectral and angular matching of the radiation properties of emitter and absorber. In TPV systems, thermal radiation from a high temperature emitter has to be spectrally matched to the bandgap of the photovoltaic (PV) cell, enabling efficient conversion

[a] *Research Laboratory of Electronics, Massachusetts Institute of Technology, Cambridge, Massachusetts, USA.*
[b] *Institute of Soldier Nanotechnologies, Massachusetts Institute of Technology, Cambridge, Massachusetts, USA.*
[c] *Department of Chemical Engineering, Massachusetts Institute of Technology, Cambridge, Massachusetts, USA.*
* *corresponding author; Fax: 1 617 253 5859; Tel: 1 617 324 6443; E-mail: vrinner@mit.edu*

into electricity. In solar thermal as well as solar TPV systems, an efficient absorber matched to the (very high temperature) solar radiation is essential. Therefore, highly selective absorbers and emitters are a critical element as a spectral conversion step in solid state thermal-to-electric energy conversion applications, which we will discuss in more detail at the end of this review as a showcase example of an application where the unique abilities of nanophotonics can achieve outstanding results. Beyond this scope, highly selective emitters/absorbers can also be applied as highly efficient infrared radiation sources and sensors for infrared spectroscopy and sensing applications, like highly selective gas and chemical sensing. [13,14]

Earlier designs for selective absorbers and emitters are based for the most part on multilayer and multimaterial structures as well as metal-dielectric composite coatings, which show restricted suitability for high temperature applications due to their limited thermal material and structural stability. In contrast, we have demonstrated – based on theory, modeling, optimization, and experimental results – that two-dimensional (2D) metallic photonic crystals (PhCs) hold immense potential for high-performance, high-temperature, spectrally and directionally selective thermal emitters. Our most recent approach presents selective emitters based on tantalum (Ta), whose inherent material properties allow for simple integration of these devices into complex systems like high temperature solid state energy conversion schemes, bringing this highly promising field one step closer to high-efficiency applications. The fabrication route we have laid out for Ta PhCs paves the way to large area selective emitters: 5 cm diameter polycrystalline substrates were used for our latest devices, and PhCs were fabricated in these substrates by standard microfabrication processes. Measurements of fabricated high aspect ratio Ta 2D PhCs show enhancement of the emissivity at wavelengths below the cut-off wavelength approaching that of blackbody, steep cut-off between high and low emissivity spectral regions, and a high level of spectral selectivity. Moreover, detailed simulations and analytical modeling show excellent agreement with experimental results.

In addition to our latest results, we will provide an overview of tungsten (W) PhC selective absorbers and emitters presented in recent years and describe a route to modeling and optimization of metallic PhCs from fundamental principles to tailor the emission properties in any desired way. An introduction to the exciting field of thermophotovoltaics as an application that is profiting immensely from the latest results in high temperature nanophotonics, enabling high efficiency solid-state high-temperature energy conversion, is presented as an outlook to the promising future of high-temperature nanophotonics.

## 2 High temperature nanophotonics

The ability to tailor the photonic density of states and thereby thermal radiation in photonic crystals allows for the efficient design of highly selective and highly efficient radiation sources. In the past, PhCs have been designed both for highly selective narrow band thermal emission with a focus on spectral, directional and polarization selectivity [11,13,15] as well as wideband thermal emissivity close to blackbody in a target wavelength range and suppressed emission otherwise. [5,16–20] Both narrowband angular [15] as well as broadband angular selectivity [21,22] can be achieved with such designs. However, in this review, we concentrate on high performance broadband selective thermal sources and absorbers with critical emphasis on obtaining the optimized broadband optical response that is necessary to provide the high power density needed in solid state energy conversion applications, while maintaining critical high temperature performance and stability. In the face of the targeted high operating temperatures ($>$1000 K) stringent challenges regarding material design have to be met, and proper material selection to prevent melting, evaporation or chemical reactions, severe minimization of any material interfaces to prevent thermochemical problems such as delamination and structural stability in the presence of surface diffusion are critical.

### 2.1 Recent achievements: Tantalum photonic crystals

Recent work on tungsten (W) photonic crystals [16,20,22–25] for high temperature applications demonstrated very promising results regarding selective thermal emitters. In our most recent work however, we try to tackle some of the shortcomings of tungsten (e. g. W is extremely difficult to weld, impeding successful system integration) from a materials research point of view and broaden the range of substrate materials used for high temperature photonic applications, and demonstrate how the substrate and its properties can be tailored to meet to the specific needs of the application, including optical, mechanical, and thermo-mechanical properties.

In particular, we use polycrystalline Ta as a substrate, which has a high melting point (3290 K) and low vapor pressure similar to tungsten as well as good intrinsic selective emissivity, with a long wavelength emissivity even below that of W. Moreover, Ta is weldable and machinable, which allows for easy integration into any device design e. g. for energy conversion applications. The concept demonstrated here however, can be extended to other refractory metals as well as their alloys, like tantalum-tungsten, which allows to tailor the mechanical, chemical, electrical, optical and thermo-mechanical substrate properties according to the system requirements.

In Fig. 1 the simulated spectral emission of a Ta PhC at normal angle, optimized for a cut-off wavelength of $\lambda_{PV} = 2.3\ \mu$m

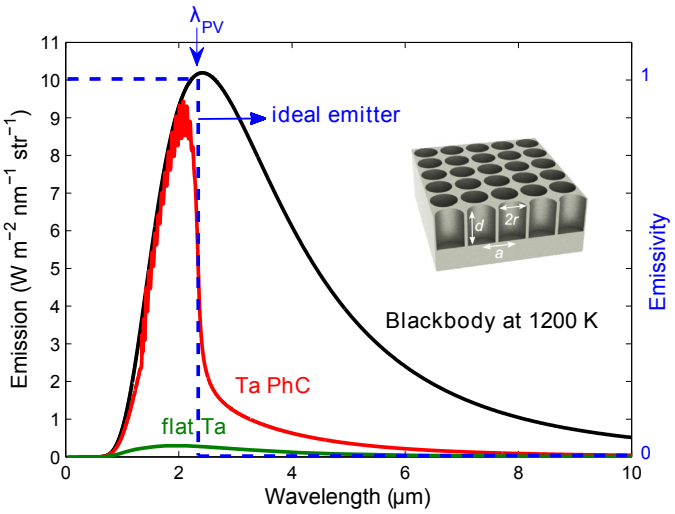


**Fig. 1** (a) Simulated normal spectral emission at 1200 K of a Ta PhC optimized for a cutoff wavelength of $\lambda = 2.3\mu$m (red) with radius $r = 0.62\mu$m, a period $a = 1.35\mu$m and an etch depth of $d = 14.95\mu$m compared to that of flat Ta (green) and that of a blackbody emitter (black), and the emissivity of an ideal emitter (blue dashed line). Inset: schematic view of the PhC.

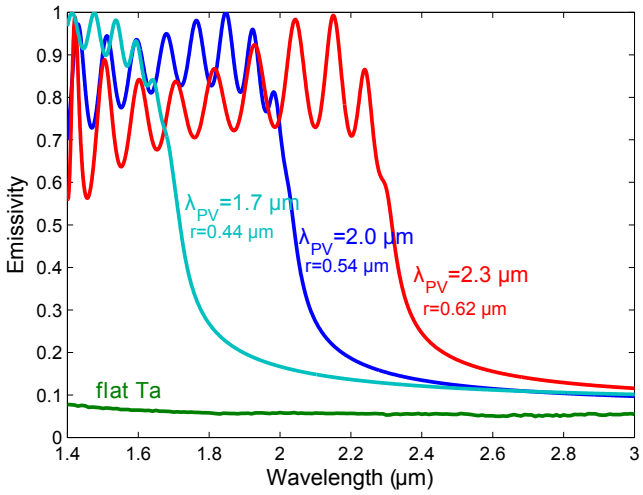


**Fig. 2** Simulated normal emissivity of a Ta PhC optimized for a cut-off wavelength of $\lambda$= 2.3 $\mu$m (red), $\lambda$= 2.0 $\mu$m (blue) and $\lambda$= 1.7 $\mu$m (light blue) with the etch depth $d$ restricted to 8 $\mu$m as compared to the emissivity of flat Ta (green).

is compared to the emission of flat Ta[26] and blackbody emission at 1200 K. We employ a finite difference time domain (FDTD) algorithm[27] implemented via MEEP,[28] a freely available software package developed at MIT, for simulation of the optical properties of the PhCs, which are designed as a square array of circular cavities with a period $a$, radius $r$ and cavity depth $d$ etched into the substrate (see inset in Fig. 1). The optical dispersion relation of Ta is incorporated in the simulations via a Lorentz-Drude oscillator model, whose parameters are fitted to the experimentally measured reflectance of flat polished Ta. By matching the quality (Q) factors of the radiative and absorbing modes of the cavities of the PhC,[25,29] the emission below the cut-off wavelength is greatly increased from the intrinsic emission of flat Ta, approaching that of a blackbody. At the same time, the emission at wavelengths above the cut-off is kept low, approaching that of the bare substrate for long wavelengths (above 6 $\mu$m), minimizing losses due to waste heat and achieving high selectivity.

The optimized parameters of this PhC, designed for a cut-off wavelength of $\lambda_{PV}$= 2.3 $\mu$m are a cavity radius of $r$= 0.62 $\mu$m, a period $a$= 1.35 $\mu$m and an etch depth of $d$= 14.95 $\mu$m. As the emissivity of bare Ta below this cut-off wavelength is low, the PhC needs deep cavities to allow for a high quality factor Q of the fundamental cavity resonant mode, and a long interaction time of the radiation in this mode to be efficiently absorbed. With this design, a normal spectral efficiency (i. e. the ratio of useful emitted power below the cut-off wavelength to the total emitted power at a given temperature) of 66.7% can be achieved at 1200 K. For a greybody the spectral efficiency is typically less than about 35%, in particular for flat Ta it is 31.5% at 1200 K. At the same time, the total amount of useful emission below cut-off is increased to 726.7 mW/cm$^2$ for the optimized Ta PhC at normal angle, as opposed to only 29.6 mW/cm$^2$ for a flat Ta substrate.

The simulated emissivity of Ta PhC optimized for a different cut-off wavelengths of $\lambda_{PV}$ = 1.7, 2.0 and 2.3 $\mu$m and that of flat Ta (as obtained from measured reflectivity of a flat polished substrate at room temperature) is shown in Fig. 2. Here, the etch depth of the cavities was limited to 8 $\mu$m to facilitate fabrication. Simulations have shown that for increased cavity depth above about $d$=8.0 $\mu$m, the increase of emissivity below the cut-off is diminishing. A sharp cut-off between the high emissivity range approaching unity and the low emissivity range, limited by the intrinsic emissivity of Ta, can be achieved for all of these designs. The flexible design approach based on the fundamental principles of the PhC[25,29] allows for efficient tailoring of the cut-off wavelength to match the desired bandgap $\lambda_{PV}$ of the PV cell.

To demonstrate the viability of this approach, we have fabricated Ta PhCs according to our optimized design using a process similar to that used for W PhCs[24,25] and further evolved and optimized for Ta substrates. We use large grain polycrystalline Ta, which is more affordable and readily available even as large area substrates as opposed to single crystal substrates, making large-area applications feasible. Substrates of 1.9 cm and 5 cm diameter were used to fabricate selective emitters for

a radioisotope TPV application.

The polycrystalline substrates were annealed at 2250°C in vaccum to enhance thermal stability of the grains and minimize grain boundary diffusion at high operating temperatures, and subsequently lapped and polished to an optical degree with a surface roughness $R_a < 1$ nm. The fabrication of the PhCs involves the steps of pattern definition by interference lithography (IL) based on a trilayer resist process[30], defining the final cavity diameter by ashing of the photoresist and antireflective coatings, pattern transfer to a thin chrome (Cr) hard mask by reactive ion etching (RIE), and the final etching of the substrate by deep reactive ion etching (DRIE) using an $SF_6$ based Bosch process. With this etch process we have been able to achieve up to 7$\mu$m deep cavities with an aspect ratio of 5, steep sidewalls and negligible sidewall roughness (see Fig. 3a). The selectivity of the Ta etch is high enough that 120 nm of Cr hard mask is sufficient for this etch depth, and the etching of the Cr hard mask is negligible. As we employ achromatic interference lithography on a Mach-Zehnder setup[31] the fabrication scheme is easily scalable to large area substrates while maintaining long range fabrication precision over large areas. Fabricated samples show impressive uniformity of the optical properties over the sample surface of up to 5 cm in diameter (Fig. 3a). In another approach, we have also successfully used contact photolithography to achieve large area pattern definition of the 2D PhC.

The spectral emissivity of fabricated Ta PhCs, as obtained from near normal incidence reflectivity measurements at room temperature, is shown in Fig. 3b. The specular reflectivity $R$ was measured with an OL750 spectroradiometer in the range of 1-3 $\mu$m. For the opaque samples, the emissivity $E$ is given by $E = 1 - R$. Note that diffraction, which occurs below a wavelength corresponding to the period of the PhC and increases the total reflection, is not captured by this method. As can be seen in Fig. 3b, a sharp cutoff between high and low emissivity regions and very good agreement with simulation results (as obtained from FDTD simulations) is achieved. Studies of the influence of various fabrication imperfections show that in this case, the slight broadening of the cutoff and increase of the emissivity above the cutoff wavelength is mostly due to a slight tapering of the sidewalls. Sidewall disorder, i. e. random roughness of the cavity edge can be neglected due to our optimized dry etch process of the Cr hard mask, which allows for precise control of the cavity diameter and smooth edges as compared to a wet etch process (as previously used for W PhCs[24,25]). Also, we ensured by Auger electron spectroscopy (AES) that there is no contamination from the Cr hard mask after removal of the etch mask, which would be detrimental to the desired low emissivity at long wavelengths. Preliminary investigation of the spectral emission at elevated temperatures measurements show that the emission of the fabricated Ta selective emitters is stable at a heater tem-

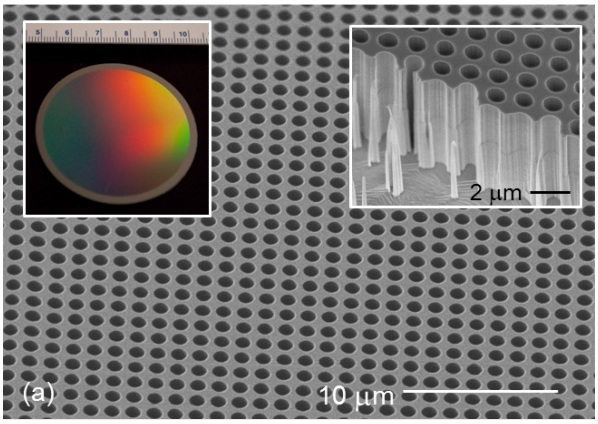


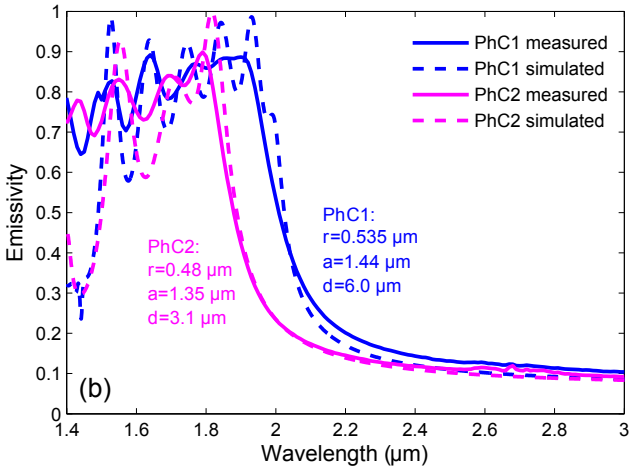


**Fig. 3** (a) Scanning electron micrograph of fabricated Ta PhC (sample PhC1 with radius $r = 0.535\mu$m, a period $a = 1.44\mu$m and an etch depth of about $d = 6\mu$m) showing excellent fabrication accuracy and long range fabrication uniformity. Left inset: Digital photo of the full 5 cm diameter substrate after etching of the Cr hard mask (scale is in cm). Right inset: Scanning electron micrograph of the cross sectional view of the etched Ta PhC. (b) Measured normal room temperature emissivity of two samples of fabricated Ta PhCs (solid lines) with different cut-off wavelengths as compared to simulation (dashed lines).

perature of 1000°C for more than an hour. Further evaluation of the spectral emission and high temperature stability is under way. These results confirm the viability and performance of Ta based PhCs as selective emitters and absorbers opening a new path to high efficiency high temperature nanophotonic devices tailored for applications in energy conversion schemes.

### 2.2 Tungsten selective emitters

One approach to spectrally selective emitters/absorbers encompasses multilayer stacks and multimaterial structures.[21,32–35] However, the usage of multiple materials is detrimental to stable performance at high operating temperatures as discussed above, due to thermochemical stresses between the materials and chemical reactions initiated at elevated temperatures. Also, more elaborate 3D PhCs fabricated by layer-by-layer or other techniques like templated electrodeposition contain multiple interfaces prone to thermal degradation.[18,36,37] Early studies exist regarding thermal degradation by surface diffusion and enhancing thermal stability by additional surface coatings.[37,38] For thermal stability and high performance at elevated temperatures it is most advantageous to use all-metallic 2D PhCs which reduces the number of interfaces. In particular, refractory metals exhibit low emissivity at long wavelengths (i. e. above $\sim 2.5\mu$m) and increasing emissivity in the near infrared, in addition to high melting points ($>$ 3000 K) and low vapor pressure. This low emissivity at long wavelengths is vital for selective emitters for energy conversion applications like TPV, since longer wavelength emission is generally below the bandgap of the current state of the art low bandgap TPV cells, and lost as waste heat. The increased emissivity below $\sim 2.5\mu$m due to interband transitions on the other hand enables us to easily enhance emission in the wavelength range important for TPV energy conversion. This intrinsic wavelength selectivity is also necessary for application as an efficient solar selective absorber characterized by strong solar absorption and low thermal emissivity, as will be discussed below. Most promising designs aiming at spectral selectivity have been proposed on the basis of 2D surface structured tungsten, with notable results both in theory as well as experiment.[16,20,22–25]

In one interesting approach, S. Fan and co-workers have presented a selective absorber based on a periodic array of tungsten pyramids, with spectral selectivity over a broad angular band (for incident angles up to 60°).[22] This design is based on impedance matching of the incident wave by a gradual adiabatic change of the effective refractive index of the substrate. A solar TPV system using this absorber in conjunction with a large area selective emitter has been proposed, with the potential to exceed the Shockley-Queisser limit[39] of 41% efficiency under full concentration of sunlight, using a 0.7 eV PV cell under high sun concentration (about 2000 suns) and assuming a high area ratio (more than 16) for the absorber/emitter pair.[17]

In a different approach a 2D photonic crystal can be designed so as to match the edge of its optical bandgap to the desired cutoff wavelength of the emissivity, as presented above for Ta. Both selective emitters and absorbers made of W have been presented based on this approach.[20,40,41] Based on a 2D array of cylindrical cavities in W, an optimized design for broadband angular and spectral selectivity of a solar absorber was recently presented.[41] Such an absorber operating at 1,000 K and employing 100 sun concentration yields a thermal transfer efficiency of 74.1%. In this study, the tremendous impact of the spectral and angular selectivity of the absorber on the overall energy conversion efficiency of a solar TPV system was demonstrated, taking into account all system parameters of cut-off frequencies, acceptance angles, absorber/emitter ratio, TPV bandgap and temperature.[41] It could be shown that incorporating angular selectivity to the absorber, even using typical values for spectral selectivity and unconcentrated sunlight, the system efficiency can be increased to 37% as opposed to merely 10.5% for a typical spectrally selective absorber without angular selectivity. This result would also exceed the Shockley-Queisser limit[39] of 31% efficiency without concentration of sunlight.

Also, a highly selective emitter based on a tungsten 2D PhC was recently proposed, following the design route for metallic 2D PhC selective emitters as presented below. It was fabricated on a 1 cm diameter singlecrystal substrate and its high temperature emission properties were characterized.[24,25] It exhibited short wavelength emissivity reaching that of a blackbody emitter, broadband low emissivity at long wavelengths and a sharp cut-off between the two regions, offering an exceptional emissivity contrast of 4:1 over 10% wavelength separation. A fabrication route to obtain uniform fabrication while maintaining nanoscale accuracy was described, and thermal emission measurements at high temperatures ($\sim$1200 K) of fabricated samples have demonstrated its exceptional high temperature performance (see Fig. 4).

### 2.3 Design and modeling of metallic PhCs

Understanding the optical properties of 2D photonic crystals enables us to engineer their spectral and directional emissivity and to design structures with a tailored selectivity. The most simple design comprises a square array of cylindrical cavities with period $a$, radius $r$, and depth $d$ etched into a uniform substrate,[20] and the basic principles and mechanisms leading to spectral selectivity can be readily understood and exploited to achieve a desired cut-off wavelength.

In general, the enhancement in emissivity is achieved by coupling into resonant electromagnetic modes of the cavity, whereby the cut-off wavelength is approximately given by the fundamental mode of the cylindrical metallic cavity.[20,23,42]

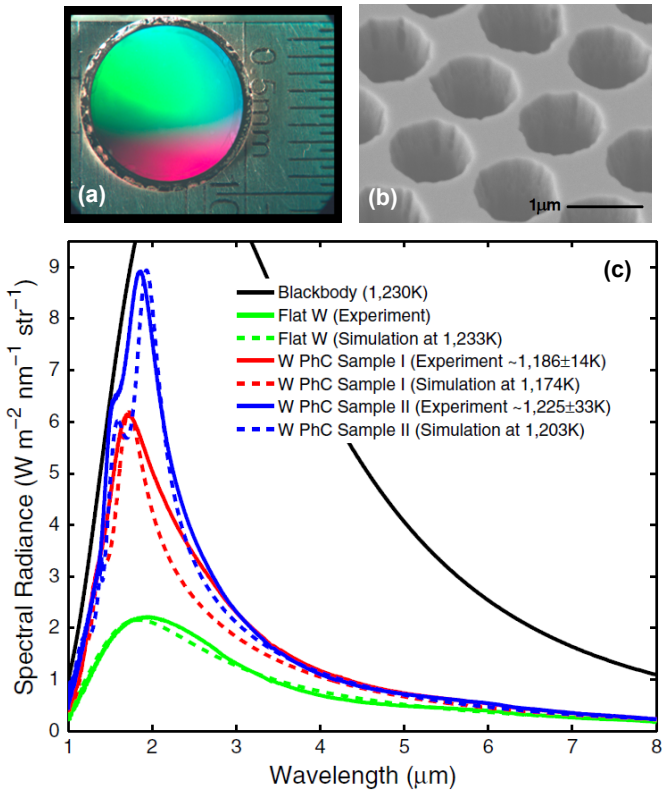


**Fig. 4** Fabricated W PhC (Yeng et al.[25]): (a) Digital photo of the fabricated 1 cm diameter sample and (b) Scanning electron micrograph of the fabricated W PhC. (c) Measured and simulated normal spectral emission obtained by heating the samples to ∼1200 K as compared to emission from flat W (green) and ideal blackbody emission (black).

For radiation with wavelengths shorter than the fundamental cavity resonant wavelength, enhanced absorption occurs due to the increased interaction time with the absorptive metal. (Note that via Kirchhoff's law of thermal radiation, emissivity and absorption must be equal at every wavelength.[43]) On the other hand, there are no modes to couple to for radiation with wavelengths longer than the fundamental cavity resonant mode, thus achieving the desired wavelength selectivity. Using these guidelines, we can tailor the cut-off wavelength by selecting the appropriate $r$ and $d$ as a first step. To further enhance the selective emitter's performance, we have developed an analytical approach based on coupled-mode theory[44] to select the appropriate $r$, $d$, and $a$.[25,29] Following this approach, the maximum emissivity below the desired cut-off wavelength is achieved when the radiative and absorbing quality factors $Q_{rad}$ and $Q_{abs}$ of the photonic crystal cavity resonances are matched. In this case, the interaction time of light is long enough to be absorbed efficiently. For $Q_{rad}>Q_{abs}$ the radiation is undercoupled to the cavity modes and free space radiation does not sufficiently enter the cavity, resulting in less than optimal absorption. For $Q_{rad}<Q_{abs}$ on the other hand, free space radiation is overcoupled to the PhC cavity resonances, and light is radiated back into free space before it can be absorbed. The first step in optimizing the PhC design for maximum peak emissivity therefore is to compute the quality factors $Q_{rad}$ and $Q_{abs}$ of the cavity, and to optimize the cavity parameters (radius $r$ and depth $d$) to achieve Q-matching. Following the analysis in Ghebrebrhan et al.[29] it is found that for a particular cut-off wavelength, an optimal pair of $r$ and $d$ exists. The period $a$ has a significant influence on the emissivity only at wavelengths close to or smaller than the periodicity, whereupon diffracted plane waves and surface plasmon modes start to appear. Because the emissivity enhancement is dominated by the Q-matched electromagnetic cavity modes, surface plasmons can be neglected in the analysis.[29] In contrast, diffractive modes decrease the emissivity below the cut-off, as higher-order resonances may couple into multiple channels corresponding to diffraction, thus increasing total reflectivity. To achieve the intended broadband emissivity enhancement it is therefore important to choose the smallest period possible for a fixed radius, such that multiple resonances only re-emit back into the incident channel (i. e. above the diffraction limit). The period $a$ is then limited only by the sidewall thickness that must be thicker than the skin-depth of the metal to preserve the wavelength selectivity of the emitter, and thick enough to facilitate fabrication.

With this first design choice of parameters, obtained for a particular cut-off wavelength by Q-matching, the electromagnetic properties of a periodic array of cavities can be computed by numerical simulations, and the parameters of the PhC further optimized to achieve the desired selectivity. The maximum of a target function (i. e. system efficiency) can be found by a global optimization algorithm including all optimization parameters (as described in Bermel et al.[40]). We use MEEP, a finite difference time domain (FDTD)[27] simulation algorithm developed at MIT[28] to calculate the reflectivity and absorption (their sum amounting to unity) of the optimized PhC. Note that this calculation method is exact apart from the approximations of material dispersions (which is included in the calculation by a Lorentz-Drude oszillator model) and grid discretization.

As the magnitude of the first emissivity peak in the first instance is controlled solely by Q-matching, this design route is directly applicable to PhCs made of any highly reflective metallic material (e. g. platinum, silver, tungsten, tantalum, or alloys), allowing us to tailor the substrate properties according to the requirements of the application. As discussed above, refractory metals are particularly advantageous as they exhibit both high melting point and low vapor pressure, which makes them particularly suitable for very high temperature applications with proper vacuum packaging.

## 3 Emerging applications: Thermophotovoltaic energy conversion

More than 92% of the world's primary energy sources (i. e. fossil fuels and nuclear energy) are converted into electrical and mechanical energy through thermal processes, and solar energy is fundamentally a high temperature (∼5800 K) heat source. As the majority of energy production and conversion is at some stage transformed into thermal energy, understanding and being able to manipulate and convert thermal directly into electrical energy opens numerous possiblities, eliminating other more lossy conversion stages, or using heat that is otherwise lost as waste heat in a variety of processes to gain back valuably energy. TPV energy conversion was first proposed in 1960's.[45,46] It is a direct thermal to electric energy conversion scheme, whereby photons produced by a thermal emitter drive a suitable low-bandgap photovoltaic (PV) cell. This concept permits direct thermal to electrical energy conversion without any mechanical components and on small device scales, i. e. with high power densities, fundamentally limited only by Planck's blackbody law. In a photovoltaic system, the efficiency is limited due to the mismatch of the radiation spectrum and the spectral properties of the PV diode: Photons with energies below the bandgap do not contribute to the electrical current, and for each high energy photon, the energy in excess of the bandgap is dissipated as waste heat (phonons) and thus lost in the sense of power conversion. The efficiency of any TPV system therefore depends on the careful match of the emitter spectrum to the electronic bandgap and spectral properties of the PV material, and can be tremendously increased by the use of spectrally selective emitters.

The TPV approach is schematically illustrated in Fig. 5. The thermal energy from any heat source is used to heat a selective emitter, which emits photons preferably in a narrow bandwidth $\Delta\lambda$ below the bandgap $\lambda_{PV}$ of the PV cell. A (cold side) filter in front of the PV cell can be used to additionally narrow down the spectrum and reflect any low energy photons, which are re-absorbed by the selective emitter, while transmitting most of the useful high energy photons.

The efficiency of the TPV system as illustrated in Fig. 5 depends on the operating temperature of the system, which defines the energy of the maximum emission according to Planck's law, the energetic position of the bandgap of the PV cell and its external quantum efficiency, and the spectral selectivity of the emitter and the filter, if applied. In a realistic system, additional losses due to thermal conduction and convection as well as side losses have to be taken into account, and can be amended for by proper system design, vacuum packaging and a high view factor, i. e. small distance between the emitter and the PV cell.

Regarding the spectral match of the peak emission to the PV cell, TPV energy conversion is profiting tremendously

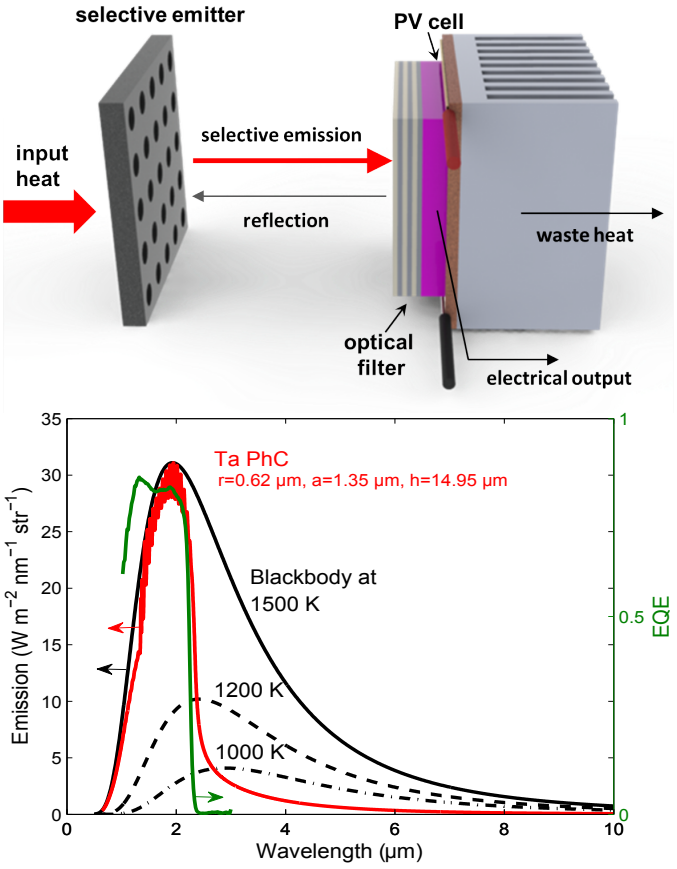


**Fig. 5** Concept of the thermophotovoltaic approach using a spectrally selective emitter matched to the bandgap $\lambda_{PV}$ of the PV cell. Below: Thermal emission of an ideal blackbody at different temperatures T as compared to the emission of a Ta PhC selective emitter (red) optimized for a cut-off wavelength $\lambda_{PV}$ =2.3 $\mu$m, and the external quantum efficiency of a quartenary InGaAsSb PV cell (green) with a bandgap $E_g$=0.52 eV (∼ $\lambda_{PV}$ =2.3 $\mu$m).[47]

from the research advancements and the availability of narrow gap semiconductors for photodiode fabrication (e. g. Ge with 0.66 eV, GaSb with 0.72 eV, InGaAs with 0.6 eV and GaInAsSb with 0.53 eV), pushing the ideal cut-off wavelength of the emitter to longer wavelengths. Different TPV systems based on GaSb[48,49], InGaAs[50–52] and quartenary InGaAsSb[47,53–55] diodes as well as thin film CIGS photocells[56] have been proposed and demonstrated. The narrow bandgaps of these alternative diode materials allow for a higher spectral overlap between the emitter and the diode material, even at lower emitter temperatures. To reach a maximum emission at the bandgap wavelength, high operating temperatures are necessary - the maximum emission of an ideal blackbody being at about 2.5 $\mu$m ($\sim$0.5 eV) at 1200 K and at about 2.0 $\mu$m ($\sim$0.62 eV) at 1500 K (Fig. 5 bottom). The high operating temperatures impose strict requirements on the material properties and thermal stability of the selective emitter used. With new achievements in material and device engineering for all-metallic 2D PhC selective emitters as discussed above, TPV systems have advanced to high temperature devices, with long-term operation stability at temperatures well above 1200 K becoming feasible. This is a critical advancement in the field of solid state thermal-to-electrical energy conversion. Also, with such highly selective emitters, a decent efficiency even at lower operating temperatures can be achieved.

TPV has proven to be an extremely versatile energy production and conversion concept, as it can be employed to convert energy of any thermal source into electrical energy. Thus, a variety of applications have been proposed, encompassing combustion TPV,[57–59] radioisotope TPV[60] as well as solar TPV,[61] solar thermal and solar chemical applications[62] (Fig. 6) with highly promising key figures such as efficiency, power density and output power. In comparison to conventional thermal to electrical energy conversion by mechanical engines, the TPV concept offers the advantage of versatility of the 'fuel', higher reliability and less maintenance requirements due to the absence of moving parts, and the potential for smaller form factors and higher power densities. Indeed a micro-TPV system with a 1 cm$^2$ microreactor operating at 850°C and an output power of 150 mW has been proposed and demonstrated.[57] Radioisotope TPV applications are used with radioisotope fuel cells, and allow for a very robust and stable energy source for long-term operation (18-30 years) in extreme environments, therefore ideal for space applications but also for terrestrial energy supply where other energy sources are not available or stable long-term operations is needed.

Another promising technology that can potentially beat the Shockley-Queisser limit[39] is solar TPV, where the expected efficiencies and key figures have been particularly well studied.[63–65] In the solar TPV system, (concentrated) solar radiation is absorbed by a selective absorber and used to heat a

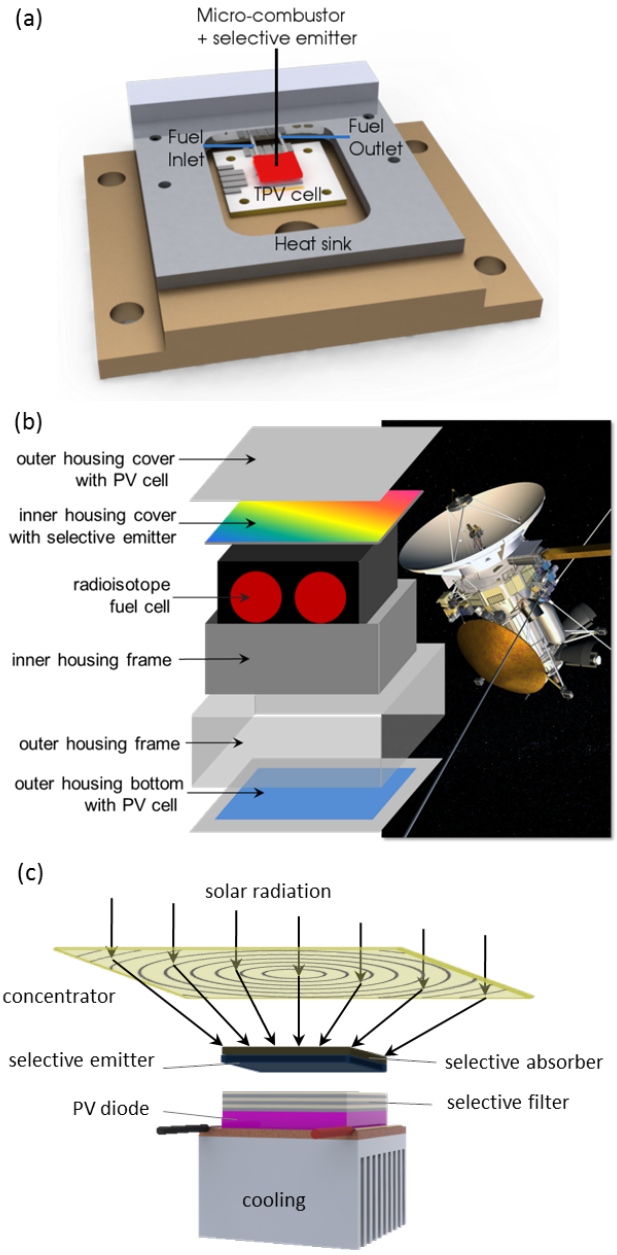


**Fig. 6** TPV applications using different thermal sources: Combustion TPV (top) using hydrocarbon fuel, radioisotope TPV using heat from radioactive decay (center), and solar TPV (bottom).

selective emitter. This combined absorber/emitter structure can be designed to efficiently absorb broadband solar radiation and convert it to suitable narrow-band emission matching the bandgap of the PV cell.

The absorber ideal for solar-thermal as well as solar TPV energy conversion has to absorb any radiation of wavelengths below a cut-off and exhibit completely suppressed emission above this wavelength in order to prevent energy losses by re-emission of photons. Therefore, a step-function profile is targeted for the absorptivity characteristics of an ideal absorber, where the position of the cut-off wavelength depends on the absorber temperature and the solar concentration factor, as a balance between the long wavelengths portion of the solar spectrum that is not absorbed and the losses by re-emission of the absorber has to be established. To keep these losses low, the cut-off wavelength has to be shifted towards shorter wavelengths with increasing operation temperature, compensating the blue-shift of the blackbody emission with rising temperature.[21]

A number of material types have been studied for solar thermal and early solar TPV applications, among them intrinsically selective materials (materials intrinsically exhibiting spectrally selective absorption to some extent), metal-dielectric composites (cermets), semiconductor- metal tandems, multilayer absorbers and surface structured metals[66] - but none of them are stable at the elevated temperatures required for high efficiency solar TPV or solar thermal applications. As discussed above, the use of metallic 2D PhCs for selective absorption and emission is particularly advantageous and opens up the possibility for efficient high temperature operation. In addition to the spectral match of the incident photons to the bandgap of the PV cell, losses from radiative recombination in the PV cell can be reduced in a TPV system: photons radiated from the PV cell in unwanted radiative electron-hole recombination processes can be recycled by the TPV system as they are re-absorbed by the emitter.[65,67] Therefore, the PV cell can be operated close to open-circuit condition, whereas a conventional PV system has to be operated at its maximum power point at lower voltage, in order to minimize the losses caused by radiative recombination in the PV cell. In the case of an optimal design for this intermediate step, the efficiency of a solar thermal TPV system can even exceed that of single-junction PV cells. It has been predicted that the theoretical efficiency limit of a solar TPV system can surpass the Shockley-Queisser limit[39] for a single-junction solar cell, stating that the maximum efficiency of a single-junction solar cell cannot exceed 31% without and 41% under full concentration of sunlight. In contrast solar TPV systems can have theoretical efficiencies of up to 54% without and 85% under full concentration of sunlight[65,67] which is very close to the theoretical limit for a tandem configuration of infinitely many PV cells with different bandgaps of 86.8%.[68]

For any TPV applications, the careful design of the selective emitter or absorber/emitter regarding high optical selectivity, while considering their material and structural stability at high operating temperatures, is the key to obtaining the high efficiencies and impressive key figures proposed by theoretical studies.

## 4 Conclusions

In recent years, research in the field of high temperature nanophotonics has brought forward a number of very interesting approaches for selective emitters, the crucial component to boost the efficiency and thereby proof the viability of novel high temperature thermal-to-electrical energy conversion schemes. In particular, most promising approaches to spectrally and directionally controlled thermal radiation so far have been based on 2D surface structured tungsten, due to its high thermal stability and intrinsic selective emissivity, and a number of selective tungsten emitters and absorbers have been demonstrated both in theory as well as practice.

In our most recent approach, we have demonstrated selective emitters based on Ta, which has superior machinability and weldability as compared to W along with the favorable thermal properties, making the selective emitters based on Ta suitable for system integration. The fabrication route presented here together with the design route for all-metallic 2D PhCs allows for a substrate choice to meet the system requirements regarding mechanical, optical, and thermo-mechanical material properties and allow system design for energy conversion on a compact one-material platform.

We have demonstrated the use of large area (5 cm diameter), large grain polycrystalline Ta substrates and a fabrication scheme based on interference lithography and dry etching (RIE), opening up a route to large area selective emitters. The fabrication process presented here also allows for upscaling to larger, wafer-sized substrates. We have presented deep cavity Ta resonators etched by an optimized Bosch process obtaining an aspect ratio of up to 5, allowing for efficient coupling to the resonant cavity modes. The measured emissivity at room temperature showed excellent agreement with theory, an outstanding selective enhancement of the emissivity below the target cut-off wavelength and a steep cut-off while maintaining the low intrinsic emissivity of flat Ta above the cut-off wavelength. Preliminary results of high temperature emissivity measurements showed that the emissivity of the fabricated Ta selective emitters is stable at a heater temperature of 1000°C for more than an hour.

These promising results demonstrate the efficiency of selective emitters based on 2D photonic crystals in refractory metals. They are paving the way for novel high efficiency high temperature thermal-to-electricity conversion schemes based on selective emitters and absorbers, like thermophotovoltaic

(TPV), solar thermal and solar TPV, as well as thermal-to-chemical energy applications.

## Acknowledgements

The authors would like to thank Peter Bermel and Michael Ghebrebrhan for valuable discussions, as well as Bob Geil at the University of North Carolina for performing the DRIE of Ta, James Daley at NSL (MIT) for film deposition, and Tim Savas for assistance and training in interference lithography. Fabrication of Ta PhCs was done in part at the Nanostructures Laboratory (NSL) at MIT and at the Center for Nanoscale Systems (CNS) at Harvard University, a member of the National Nanotechnology Infrastructure Network (NNIN), which is supported by the National Science Foundation under NSF award No. ECS-0335765. This work was partially supported by by the Army Research Office through the Institute for Soldier Nanotechnologies under Contract Nos. DAAD-19-02-D0002 and W911NF-07-D000. Y. X. Y. and M. S. were partially supported by the MIT S3TEC Energy Research Frontier Center of the Department of Energy under Grant No. DE-SC0001299. V. R. acknowledges funding by the Austrian Science Fund (FWF): J3161-N20.

## References

1 E. Yablonovitch, *Physical Review Letters*, 1987, **58**, 2059.
2 S. John, *Physical Review Letters*, 1987, **58**, 2486.
3 J. D. Joannopoulos, *Nature*, 1995, **375**, 278.
4 J. D. Joannopoulos, S. G. Johnson, J. N. Winn and R. D. Meade, *Photonic Crystals: Molding the Flow of Light*, Princeton, Princeton, NJ, 2nd edn, 2008.
5 J. Fleming, S. Lin, I. El-Kady, R. Biswas and K. Ho, *Nature*, 2002, **417**, 52.
6 S. Fan, P. R. Villeneuve and J. D. Joannopoulos, *Physical Review B*, 1996, **54**, 11245–11251.
7 M. M. Sigalas, C. Chan, K. M. Ho and C. M. Soukoulis, *Physical Review B*, 1995, **52**, 1174411751.
8 E. R. Brown and O. B. McMahon, *Applied Physics Letters*, 1995, **67**, 21382140.
9 S. Lin, J. Fleming, D. L. Hetherington, B. K. Smith, R. Biswas, K. M. Ho, W. Z. M. M. Sigalas, S. R. Kurtz and J. Bur, *Nature*, 1998, **394**, 251.
10 C. M. Cornelius and J. P. Dowling, *Physical Review A*, 1999, **59**, 47364746.
11 J. J. Greffet, R. Carminati, K. Joulain, J. P. Mulet, S. Mainguy and Y. Chen, *Nature*, 2002, **416**, 61.
12 F. Marquier, K. Joulain, J. P. Mulet, R. Carminati and J. J. Greffet, *Optics Communications*, 2004, **237**, 379.
13 M. U. Pralle, N. Moelders, M. P. McNeal, I. Puscasu, A. C. Greenwald, J. T. Daly, E. A. Johnson, T. George, D. S. Choi, I. El-Kady and R. Biswas, *Applied Physics Letters*, 2002, **81**, 4685.
14 N. Moelders, M. U. Pralle, M. P. McNeal, I. Puscasu, L. Last, W. Ho, A. C. Greenwald, J. T. Daly, E. A. Johnson and T. George, MRS Proceedings, 2002, p. U5.2.1.
15 I. Celanovic, D. Perreault and J. Kassakian, *Physical Review B*, 2005, **72**, 075127.
16 A. Heinzel, V. Boerner, A. Gombert, B. Blasi, V. Wittwer and J. Luther, *Journal of Modern Optics*, 2000, **47**, year.
17 E. Rephaeli and S. Fan, *Optics Express*, 2009, **17**, 15145.
18 S. Y. Lin, J. Moreno and J. G. Fleming, *Applied Physics Letters*, 2003, **83**, 380 –382.
19 H. Sai, Y. Kanamori and H. Yugami, *Applied Physics Letters*, 2003, **82**, 1685–1687.
20 I. Celanovic, N. Jovanovic and J. Kassakian, *Applied Physics Letters*, 2008, **92**, 193101.
21 N. P. Sergeant, O. Pincon, M. Agrawal and P. Peumans, *Optics Express*, 2009, **17**, 22800.
22 E. Rephaeli and S. Fan, *Applied Physics Letters*, 2008, **92**, 211107.
23 H. Sai and H. Yugami, *Applied Physics Letters*, 2004, **85**, 3399.
24 M. Araghchini, Y. X. Yeng, N. Jovanovic, P. Bermel, L. A. Kolodziejski, M. Soljacic, I. Celanovic and J. D. Joannopoulos, *Journal of Vacuum Science & Technology B*, 2011, **29**, 061402.
25 Y. X. Yeng, M. Ghebrebrhan, P. Bermel, W. R. Chan, J. D. Joannopoulos, M. Soljacic and I. Celanovic, *Proceedings of the National Academy of Sciences*, 2012, **109**, 2280–2285.
26 E. D. Palik, in *Handbook of Optical Constants of Solids*, Elsevier, 1998, vol. 2, pp. 408–420.
27 A. Taflove and S. C. Hagness, *Computational Electrodynamics: The Finite-Difference Time-Domain Method*, Artech House, Boston, 2000.
28 A. F. Oskooi, D. Roundy, M. Ibanescu, P. Bermel, J. Joannopoulos and S. G. Johnson, *Computer Physics Communications*, 2010, **181**, 687 – 702.
29 M. Ghebrebrhan, P. Bermel, Y. X. Yeng, I. Celanovic, M. Soljacic and J. D. Joannopoulos, *Physical Review A*, 2011, **83**, 033810.
30 M. L. Schattenburg, R. J. Aucoin and R. C. Fleming, *J. Vac. Sci. Technol. B*, 1995, **13**, 3007.
31 A. Yen, E. H. Anderson, R. A. Ghanbari, M. L. Schattenburg and H. I. Smith, *Applied Optics*, 1992, **31**, 4540–4545.
32 N. P. Sergeant, M. Agrawal and P. Peumans, *Optics Express*, 2010, **18**, 5525.
33 F. O'Sullivan, I. Celanovic, N. Jovanovic, J. Kassakian, S. Akiyama and K. Wada, *Journal of Applied Physics*, 2005, **97**, 033529.
34 I. Celanovic, F. O'Sullivan, M. Ilak, J. Kassakian and D. Perreault, *Optics Letters*, 2004, **29**, 863.
35 A. Narayanaswamy and G. Chen, *Physical Review B*, 2004, **70**, 125101.
36 T. A. Walsh, J. A. Bur, Y. S. Kim, T. M. Lu and S. Y. Lin, *Journal of the Optical Society of America B*, 2009, **26**, 1450.
37 K. A. Arpin, M. D. Losego and P. Braun, *Chemistry of Materials*, 2011, **23**, 4783.
38 C. Schlemmer, J. Aschaber, V. Boerner and J. Luther, Proceedings of the 5th Conference on Thermophotovoltaic Generation of Electricity, 2003, p. 164.
39 W. Shockley and H. J. Queisser, *Journal of Applied Physics*, 1961, **32**, 510.
40 P. Bermel, M. Ghebrebrhan, W. Chan, Y. X. Yeng, M. Araghchini, R. Hamam, C. H. Marton, K. F. Jensen, M. Soljacic, J. D. Joannopoulos, S. G. Johnson and I. Celanovic, *Optics Express*, 2010, **18**, A314–A334.
41 P. Bermel, M. Ghebrebrhan, M. Harradon, Y. X. Yeng, I. Celanovic, J. D. Joannopoulos and M. Soljacic, *Nanoscal Research Letters*, 2011, **6**, 549.
42 D. L. Chan, I. Celanovic, J. D. Joannopoulos and M. Soljacic, *Phys. Rev. A*, 2006, **74**, 064901.
43 G. B. Rybicki and A. P. Lightman, *Radiative Processes in Astrophysics*, John Wiley and Sons, New York, 1979.
44 H. A. Haus, in *Waves and Fields in Optoelectronics*, Prentice-Hall, Englewood Cliffs, NJ, 1984, p. 07632.
45 H. Kolm, *Solar-battery power source*, MIT-Lincoln Laboratory quarterly progress report, solid state research, group 35, 1956.
46 B. Wedlock, *Proc. IEEE*, 1963, **51**, 694–698.
47 M. W. Dashiell, J. F. Beausang, H. Ehsani, G. J. Nichols, D. M. Depoy,

L. R. Danielson, P. Talamo, K. D. Rahner, E. J. Brown, S. R. Burger, P. M. Fourspring, W. F. Topper, P. F. Baldasaro, C. A. Wang, R. K. Huang, M. K. Connors, G. W. Turner, Z. A. Shellenbarger, G. Taylor, J. Li, R. Martinelli, D. Donetski, S. Anikeev, G. L. Belenky and S. Luryi, *Electron Devices, IEEE Transactions on*, 2006, **53**, 2879–2891.

48 T. Schlegl, F. Dimroth, A. Ohm and A. W. Bett, Sixth Conference on Thermophotovoltaic Generation of Electricity, 2004, pp. 285–293.

49 A. W. Bett and O. V. Sulima, *Semiconductor Science and Technology*, 2003, **18**, S184.

50 B. Wernsman, R. R. Siergiej, S. D. Link, R. G. Mahorter, M. N. Palmisiano, R. J. Wehrer, R. W. Schultz, G. P. Schmuck, R. L. Messham, S. Murray, C. S. Murray, F. Newman, D. Taylor, D. M. Depoy and T. Rahmlow, *IEEE Transactions on Electron Devices*, 2004, **51**, 512–515.

51 N. Su, P. Fay, S. Sinharoy, D. Forbes and D. Scheiman, *Journal of Applied Physics*, 2007, **101**, 064511.

52 M. K. Hudait, Y. Lin, M. N. Palmisiano and S. A. Ringel, *IEEE Electron Device Letters*, 2003, **24**, 538.

53 W. Chan, R. Huang, C. A. Wang, J. Kassakian, J. D. Joannopoulos and I. Celanovic, *Sol. Energy Mater. Sol. Cells*, 2010, **94**, 509–514.

54 O. Sulima, A. Bett, M. Mauk, F. Dimroth, R. Dutta and R. Mueller, Thermophotovoltaic Conversion of Electricity, 2003.

55 C. A. Wang, H. K. Choi, S. L. Ransom, G. W. Charache, L. R. Danielson and D. M. DePoy, *Applied Physics Letters*, 1999, **75**, 1305–1307.

56 W. Durisch and B. Bitnar, *Solar Energy Materials & Solar Cells*, 2010, **94**, 960.

57 R. C. N. Pilawa-Podgurski, N. A. Pallo, W. R. Chan, D. J. Perreault and I. L. Celanovic, Applied Power Electronics Conference and Exposition (APEC), 2010 Twenty-Fifth Annual IEEE, 2010, pp. 961 –967.

58 M. Zenker, A. Heinzel, G. Stollwerck, J. Ferber and J. Luther, *IEEE Trans. Electron. Devices*, 2001, **48**, 367–376.

59 Y. Wenming, C. Siawkiang, S. Chang, X. Hong and L. Zhiwang, *Journal of Micromechanics and Microengineering*, 2005, **15**, S239.

60 C. J. Crowley, N. A. Elkouh, S. Murray and D. L. Chubb, *AIP Conference Proceedings*, 2005, **746**, 601–614.

61 V. M. Andreev, A. S. Vlasov, V. P. Khvostikov, O. A. Khvostikova, P. Y. Gazaryan, S. V. Sorokina and N. A. Sadchikov, *Journal of Solar Energy Engineering*, 2007, **129**, 298–303.

62 A. Steinfeld, *Solar Energy*, 2005, **78**, 603 – 615.

63 W. Spirkl and H. Ries, *Journal of Applied Physics*, 1985, **57**, 4409.

64 P. A. Davies and A. Luque, *Solar Energy Materials and Solar Cells*, 1994, **33**, 11 – 22.

65 N. Harder and P. Wurfel, *Semicond. Sci. Technol.*, 2003, **18**, S151.

66 C. E. Kennedy, *Review of mid- to high-temperature solar selective absorber materials*, NREL Technical Report TP-52031267, 2002.

67 A. DeVos, *Endoreversible Thermodynamics of Solar Energy Conversion*, Oxford University Press, 1992.

68 A. DeVos, *Journal of Physics D*, 1980, **13**, 839.